Current Biology 24, 385–392, February 17, 2014 ©2014 Elsevier Ltd All rights reserved http://dx.doi.org/10.1016/j.cub.2014.01.006

Article

Neural Circuit Components of the *Drosophila* OFF Motion Vision Pathway

Matthias Meier,[1,3] Etienne Serbe,[1,3] Matthew S. Maisak,[1] Jürgen Haag,[1] Barry J. Dickson,[2,4] and Alexander Borst[1,*]
[1]Department of Circuits-Computation-Models, Max Planck Institute of Neurobiology, Am Klopferspitz 18, 82152 Martinsried, Germany
[2]Research Institute of Molecular Pathology, Dr. Bohr-Gasse 7, 1030 Vienna, Austria

Summary

Background: Detecting the direction of visual motion is an essential task of the early visual system. The Reichardt detector has been proven to be a faithful description of the underlying computation in insects. A series of recent studies addressed the neural implementation of the Reichardt detector in *Drosophila* revealing the overall layout in parallel ON and OFF channels, its input neurons from the lamina (L1→ON, and L2→OFF), and the respective output neurons to the lobula plate (ON→T4, and OFF→T5). While anatomical studies showed that T4 cells receive input from L1 via Mi1 and Tm3 cells, the neurons connecting L2 to T5 cells have not been identified so far. It is, however, known that L2 contacts, among others, two neurons, called Tm2 and L4, which show a pronounced directionality in their wiring.
Results: We characterized the visual response properties of both Tm2 and L4 neurons via Ca^{2+} imaging. We found that Tm2 and L4 cells respond with an increase in activity to moving OFF edges in a direction-unselective manner. To investigate their participation in motion vision, we blocked their output while recording from downstream tangential cells in the lobula plate. Silencing of Tm2 and L4 completely abolishes the response to moving OFF edges.
Conclusions: Our results demonstrate that both cell types are essential components of the *Drosophila* OFF motion vision pathway, prior to the computation of directionality in the dendrites of T5 cells.

Introduction

The computation of motion is imperative for fundamental behaviors such as mate or prey detection, predator avoidance, and visual navigation. In the fruit fly *Drosophila*, motion cues are processed in the optic lobe, a brain area comprised of the lamina, medulla, lobula, and lobula plate, each arranged in a columnar, retinotopic fashion. Whereas photoreceptors respond to motion in a nondirectional way, wide-field tangential cells of the lobula plate depolarize to motion in their preferred direction (PD) and hyperpolarize to motion in the opposite or null direction (ND) [1, 2]. These direction-selective responses are well characterized by a mathematical model, the so-called Reichardt detector. In this model, signals from neighboring photoreceptors are multiplied after asymmetric temporal filtering [3–5]. Due to the anatomical complexity and miniscule size of the columnar neurons of the optic lobe, identification of the neural elements of the motion detection circuit has long proven difficult.

In agreement with previous suggestions based on costratification of Golgi-stained columnar cells [6, 7] and cell-unspecific activity labeling using the deoxyglucose method [8], recent studies identified two parallel motion processing streams, one leading from lamina neuron L1 via T4 cells and the other from lamina neuron L2 via T5 onto the dendrites of the tangential cells [9, 10]. Within each pathway, four subpopulations of T4 and T5 cells are tuned to one of the four cardinal directions (front to back, back to front, upward, or downward), providing direction-selective signals to four different sublayers of the lobula plate [11, 12]. Here, they become spatially integrated on the dendrites of tangential cells [12, 13]. The two pathways are functionally segregated with regard to their selectivity for contrast polarity: the L1 pathway is selectively responsive to the motion of brightness increments (ON pathway), while the L2 pathway responds selectively to the motion of brightness decrements (OFF pathway) [10, 12, 14–16]. These findings suggest that important processing steps of motion computation take place between the axon terminals of L1/L2 and the output regions of T4/T5.

For the ON pathway, a recent connectomic EM study of the fly medulla [17] not only identified two neurons, Mi1 and Tm3, as the most prominent postsynaptic targets of L1, but also showed that these cells make up for more than 90% of all input synapses on the dendrites of T4 cells. Most interestingly, the innervation of Tm3 and Mi1 on a single T4 cell is asymmetric, consistent with the preferred direction of the T4 cell, i.e., the lobula plate layer where it terminates. Because connectomic analysis has not yet reached the lobula, where the dendrites of T5 cells reside [6], the connectivity for the OFF pathway is known only within the lamina and the medulla [17–22]. Here, several cell types have been found to be postsynaptic to L2 [17, 18], i.e., L4, Tm1, and Tm2. Tm1 and Tm2 both receive synaptic input from L2 in the second layer of the medulla [17, 18] projecting to the first layer of the lobula. Within the lamina, L4 sends its processes into three neighboring columns, one into its "home" column and two into the two neighboring posterior columns [19, 20]. Within each of these columns, L4 forms reciprocal connections with L2 and with the processes of those L4s originating from other columns [19–22]. In its home column, L4 receives additional synaptic input from a lamina amacrine cell, as well as from photoreceptor R6 [21, 22], which might explain why blocking synaptic output from L2 leaves the visual responses of L4 intact [23]. Within the medulla, L4 synapses onto three Tm2 cells, one located in the home column and two in the adjacent columns located posterior in visual space [17, 18] (Figure 1A; for illustration purposes, only two neighboring columns are depicted). Based on their connectivity and anatomical layout, there are two plausible hypotheses for these cells' role in the motion detection circuit. First, Tm2 could exhibit a directional tuning for OFF motion from the front to the back, as suggested by the asymmetrical wiring between L4 and Tm2 [18]. Alternatively, Tm2 could act as one of the two input arms of the elementary OFF motion detector. In this case, Tm2 would reveal a preference for moving

[3]These authors contributed equally to this work
[4]Present address: Janelia Farm Research Campus, 19700 Helix Drive, Ashburn, VA 20147, USA
*Correspondence: borst@neuro.mpg.de

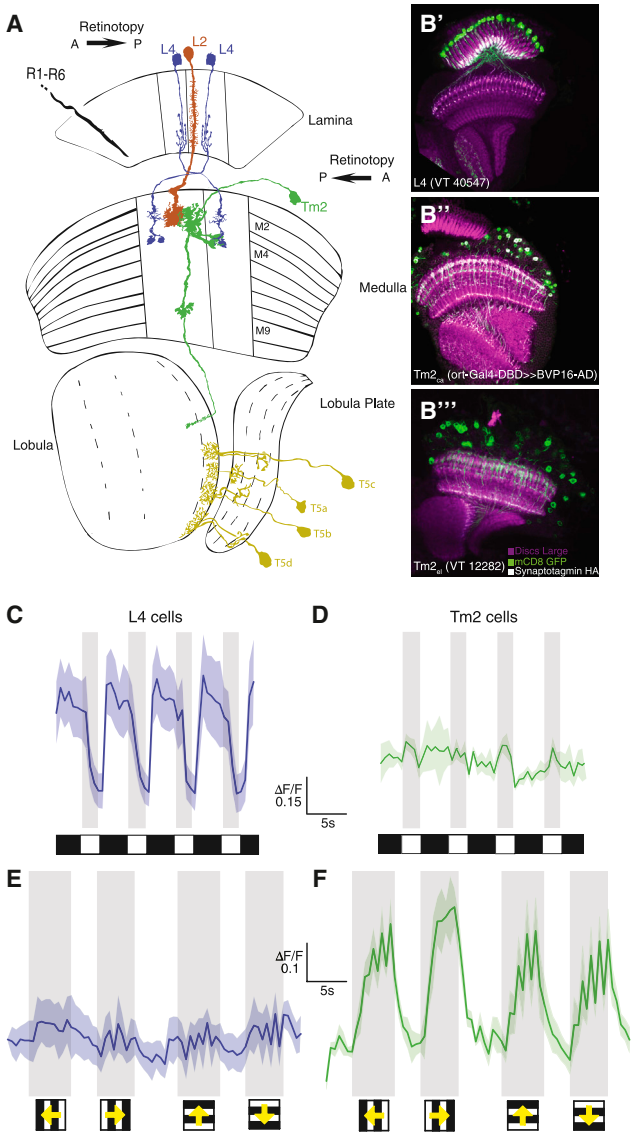

Figure 1. Wiring Diagram and Basic Response Properties of L4 and Tm2

(A) Photoreceptors (R1–R6) synapse onto the lamina monopolar cells L2 (red) and L4 (blue). These two cell types are connected in an intercolumnar and reciprocal manner in the lamina. Both give input to the transmedulla neuron Tm2 (green) in their home column. Additionally, two L4 cells from posterior columns are presynaptic to Tm2, with axonal output regions coinciding with T5 dendrites in the lobula. Adapted and modified from [6, 18].

(B) Confocal images of the Gal4-driver lines used in this study, shown in horizontal cross-sections. Neurons are marked in green (mCD8-GFP expression), neuropils in magenta (antibody against Dlg), and synaptic output regions in white (antibody against HA, bound to synaptotagmin). L4 (B′) and $Tm2_{Ca}$ (B″) lines were used for Ca^{2+} imaging. L4 (B′) and $Tm2_{el}$ (B‴) lines were used for blocking experiments.

(C and D) Average relative change of fluorescence in response to four full-field flicker stimuli in L4 (C; n = 7) and Tm2 (D; n = 5) terminals (±SEM).

(E and F) Mean responses of L4 (E; n = 7) and Tm2 (F; n = 8) to square-wave gratings moving in all four cardinal directions at 30° s^{-1}.

(C–F) Grey-shaded areas indicate the stimulation period. For Tm2, responses to vertical motion are slightly but significantly smaller than to horizontal motion ($p < 0.015$).

OFF edges, but its responses would be nondirectional; direction selectivity would only arise after a multiplicative interaction of the two input signals on the dendrites of T5 cells.

Functional analysis using behavioral readouts during selective blockade of L4 arrived at controversial conclusions: while one study found no impairment of motion-dependent behavior after silencing of L4 [23], another study observed a specific deficit in L4 block flies to detect motion from the front to the back, consistent with the first of the above hypotheses, as well as to detect moving OFF edges, consistent with the second hypothesis [24].

To probe these cells' specificity for OFF motion and their potential direction selectivity, we analyzed the visual response properties of Tm2 and L4 using Ca^{2+} imaging. Both Tm2 and L4 are excited exclusively by moving OFF edges, albeit in a non-directional way. Both cells have a bell-shaped receptive field with a half width of approximately 5°. While L4 exhibits rather linear spatial integration properties and responds to changes in full-field luminance, Tm2 becomes inhibited by stimuli of increasing size. To investigate the participation of L4 and Tm2 in motion processing, we recorded the motion responses from wide-field tangential cells, instead of using a behavioral readout. When synaptic output from either Tm2 or L4 was blocked, responses of LPTCs to moving OFF edges are eliminated, demonstrating their crucial role in the OFF pathway of *Drosophila* motion vision.

Results

To investigate the visual response properties of L4 and Tm2, we used cell-specific Gal4 driver lines. To verify these lines' specificity, we drove the expression of membrane-bound GFP and the hemagglutinin (HA)-tagged presynaptic marker protein synaptotagmin. We then antibody stained against GFP and HA, allowing us to compare the labeling with the branching as known from Golgi studies (GFP), as well as to determine the synaptic output layers (synaptotagmin). The L4 line shows specific expression of GFP within the optic lobe that is characteristic for this cell. Synaptotagmin staining of the line indicates synaptic output in the distal portion of the lamina and the second and fourth layer of the medulla, which is in agreement with previous Golgi and electron microscopy studies (Figure 1B′) [6, 17, 18]. Both of our Tm2 driver lines showed a specific, Tm2-characteristic expression within the optic lobe and similar synaptotagmin staining, labeling the ninth layer of the medulla and the first layer of the lobula (Figures 1B″ and B‴). Additional synaptotagmin label occurs in the second and fourth layer of the medulla, where EM studies have shown that Tm2 is presynaptic to L5 [17, 18]. The strong synaptotagmin staining in the first layer of the lobula suggests that this is also an output region of Tm2 where it could provide input to T5.

Visual Response Properties of L4 and Tm2

To optically record from these cells using two-photon microscopy [25], we used the $Tm2_{Ca}$ and L4 driver lines and crossed them with UAS-GCaMP5. To investigate how whole-field brightness changes are encoded in the terminals of both L4 and Tm2, we presented four spatially uniform bright pulses of light, each lasting for 2 s, interleaved by 4 s, and measured the change in fluorescence of individual L4 terminals in the second layer of the medulla and Tm2 terminals in the first layer of the lobula. In L4, the activity follows the full-field luminance in an almost tonic way, such that the lowest brightness level leads to the strongest response (Figure 1C). In contrast to L4, Tm2 does not respond to full-field luminance changes (Figure 1D). In order to test whether direction selectivity is already

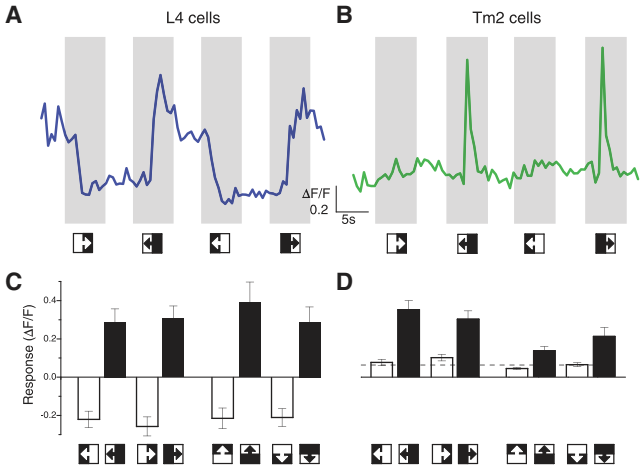

Figure 2. L4 and Tm2 Responses to Moving Edges

(A and B) Single-cell response traces of L4 (A) and Tm2 (B) to horizontally moving edges of either polarity. Stimulation period is indicated by the shaded area.

(C and D) Mean responses of L4 (C; n = 10) and Tm2 (D; n = 12) to ON (white bars) and OFF (black black) edges moving at 30° s^{-1}. Chance response level is indicated by the dashed line (see the Experimental Procedures). Error bars indicate ±SEM. For Tm2, responses to OFF edges moving in the vertical direction are significantly smaller than those for the horizontal direction ($p < 0.01$).

See also Figure S3.

present at the level of Tm2 or L4, we presented square-wave gratings moving in the four cardinal directions (back to front, front to back, upward, and downward). L4 responds with only small modulations in activity to square-wave motion (Figure 1E). In striking difference to L4, Tm2 responds strongly to gratings moving in all directions. Contradicting the hypothesis based on the asymmetric wiring in the medulla [18], Tm2 shows no directional preference, responding to gratings moving in all directions in a similar way, albeit with a somewhat smaller amplitude to vertical than to horizontal motion (Figure 1F).

Anatomical evidence has implicated both Tm2 and L4 as being postsynaptic to L2 and, thus, as potential elements in the OFF motion pathway [17, 18]. Therefore, we tested their sensitivity to the contrast polarity of moving edges. We presented either bright or dark edges, each moving in all four cardinal directions. Interestingly, L4 and Tm2 respond with quite different dynamics, as exemplified in single-cell traces in response to horizontal edge motion (Figures 2A and 2B). In L4, when an OFF edge passes the fly's visual field, the activity transiently increases settling at a plateau level that persists until the subsequent ON edge arrives. The ON edge strongly reduces L4's activity. Hence, L4 encodes moving edges with a persistent DC component, which is superimposed by a small transitory peak (Figure 2A). In contrast to L4, Tm2 responds solely with a fast, transient increase in activity to moving OFF edges (Figure 2B). When probed with moving ON and OFF edges in all directions, L4 responds to moving OFF edges equally in all four directions, primarily with a persistent change in activity. If L4's activity is at an elevated level, it becomes reduced by an ON edge (Figures 2A and 2C). As does L4, Tm2 responds to OFF edges moving in all four directions. However, in contrast to L4, Tm2 responds to moving OFF edges with a pronounced transient increase in activity. Tm2 does not respond at all to moving ON edges (Figures 2B and 2D).

To measure the receptive fields of Tm2 and L4, we periodically presented a dark vertical bar of 4.5° width on a bright background at different azimuthal positions and measured the response of both cells as defined by the difference between the relative fluorescence during bar presentation and the response level before (Figures 3A and 3B). L4 responded most strongly when the bar was within a window of about ±5° around a position, leading to maximal response (Figure 3A). The average sensitivity profile, obtained after aligning the results from different cells with respect to their maximum, closely resembles a bell-shaped Gaussian with a half width of ~5°. Tm2 responded to such stimuli in a similar way: again, maximum responses were elicited in a rather small window of about 10° widths, with no significant responses to stimulation outside this window (Figure 3B). In order to examine the spatial integration properties of L4 and Tm2, on a bright background, we presented a dark, vertical bar, increasing in size and centered at the position of a cell's maximum response. Based on L4's receptive field derived from the previous experiment and assuming linear spatial integration, we expected the responses to strongly increase with increasing bar width until approximately 10° and plateau thereafter. The response of L4 to small bar widths is consistent with this expectation; however, the response of L4 even increases when the bar width changes from 25° to 50° without any sign of saturation (Figure 3C). For Tm2, considering the data from the previous experiment (Figure 3B) and the fact that Tm2 doesn't respond to full-field flicker (Figure 1D), we expected a rather different spatial integration property. Indeed, Tm2 responses differ strongly from those of L4, displaying a maximum response to a bar of 4.5° and then decreasing rapidly as the bar becomes wider (Figure 3D). This implicates the existence of lateral inhibition, shaping the receptive field properties of Tm2.

In addition to the spatial response properties of these cells, their temporal dynamics are also of interest. Using the line-scan mode of the two-photon microscope, we measured single terminals of both cell types in response to flickering dark bars of 4.5° width at a temporal resolution of 480 Hz. As can be expected from their full-field flicker and edge responses, L4 and Tm2 responded with considerably different temporal dynamics. L4 reached its maximal response level approximately 100 ms after stimulus onset. At the end of the dark bar presentation, the fluorescence in L4 was still approximately 50% of the maximum response (Figure 3E). Tm2 responded with comparable rise times—reaching maximum response levels 100 ms after stimulus onset—but decayed much faster than L4. At the end of the bar presentation, Tm2 responses had decayed to 20% of their maximum value (Figure 3F). Note that all data obtained from Ca^{2+} imaging in layer 1 of the lobula are consistent with data from M9 (data not shown).

Motion Responses after Blocking L4 or Tm2

Our results from Ca^{2+} imaging of Tm2 and L4 cells revealed that none of these cells exhibit a preference for grating or edge motion in any direction. However, both cells become selectively excited by brightness decrease, as expected from being postsynaptic to L2. In order to assess their participation in motion processing, we blocked synaptic output of either Tm2 or L4 by expressing shibire [27] and recorded the responses of lobula plate tangential cells to moving ON and OFF edges (data from horizontal system [HS] and vertical system [VS] cells were pooled). Control flies of identical genotype but not subjected to a temperature shift showed strong and

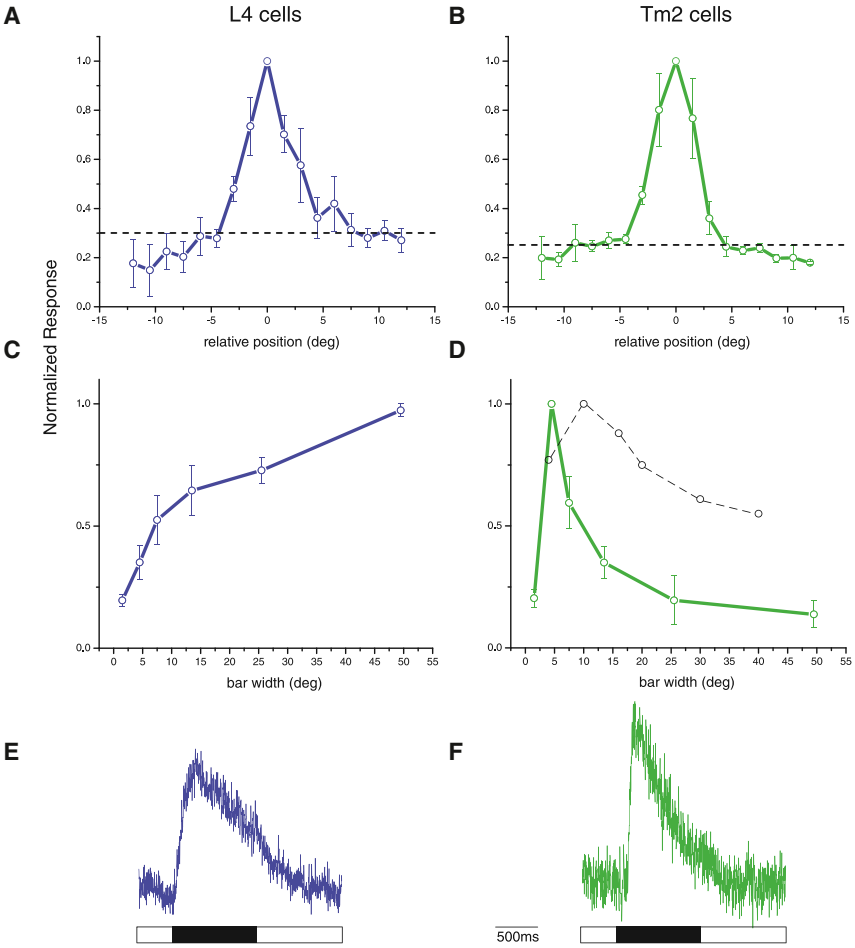

Figure 3. Response Characteristics of L4 and Tm2 Cells upon Stimulation with Flickering Bars

(A and B) Ca^{2+} response of L4 (A; n = 5) and Tm2 (B; n = 5) to 4.5°-wide, dark, vertical bars appearing and disappearing at various positions (shifted by 1.5°) on a bright background at a frequency of 0.5 Hz. Graphs were normalized to the position of the maximum response. Chance response level is indicated by the dashed line (see the Experimental Procedures). Error bars indicate ±SEM.

(C and D) Normalized Ca^{2+} response of L4 (C; n = 7) and Tm2 (D; n = 5) cells to dark, vertical bars of increasing size (bar widths: 1.5°, 4.5°, 7.5°, 13.5°, 25.5°, and 49.5°). For comparison, L2 responses from [26] are indicated as a dashed line in (D).

(E and F) Ca^{2+} response of a single L4 (E; 50 sweeps) and Tm2 (F; ten sweeps) cell (in arbitrary units) stimulated by a 4.5°-wide dark bar for 1 s, recorded at 480 Hz. The duration of the stimulation is indicated by the black bar below.

See also Figure S3.

reliable directional responses to both ON and OFF edges, depolarizing by about 8 mV during motion in the preferred direction and hyperpolarizing by about 5 mV during motion in the null direction of the tangential cells (black and gray traces in Figures 4A–4D). When L4 cells were blocked, the responses to ON edges moving along the preferred as well the null direction were almost indistinguishable from those in control flies (blue traces in Figures 4A and 4C). However, the responses to OFF edges were severely reduced, both for preferred-direction and for null-direction motion (blue traces in Figures 4B and 4D). When Tm2 was blocked, tangential cells responded strongly to ON edges moving along the preferred direction of the cells, but the response to null direction had less than half of the amplitude as compared to control flies (green traces in Figures 4A and 4C). For OFF edge motion, a similar result was obtained as for L4 block flies: Again, the response to motion along both the preferred and the null directions was almost completely abolished (green traces in Figures 4B and 4D). Using the time average of the difference between the preferred- and null-direction response as a measure, the results can be summarized as follows (Figures 4E and 4F): blocking synaptic output from L4 cells leaves the ON edge responses unaffected, but strongly and highly significantly reduces the OFF edge response (blue bars, compared to black bars); and blocking synaptic output from Tm2 cells reduces the ON edge responses somewhat, but abolishes the OFF edge response completely (green bars, compared to gray bars). A detailed comparison of preferred- and null-direction responses between control and block flies is shown in Figure S1 (available online). All of these findings are reminiscent on the results of previous studies in which either L2 or T5 cells were blocked, leading to a selective loss of tangential cell responses to OFF edges [10, 12].

We also tested the responses of L4 and Tm2 block flies to grating motion (Figure S2). As expected from the above results and the assumption that T4 and T5 cells contribute to the grating response with about equal weight, grating responses to horizontal and to vertical motion in L4 and Tm2 block flies are found to be at roughly half of the amplitude as in control flies. However, consistently in HS and VS cells, the null-direction response is compromised more strongly than is the preferred-direction response. While this might indicate a direction-specific contribution of L4 and Tm2 at first sight, it can be readily explained by a slightly elevated threshold of the inhibitory input to the tangential cells. We therefore conclude that both L4 and Tm2 cells represent essential, nondirectional components of the OFF motion pathway in *Drosophila*.

Discussion

Our results reveal that L4 and Tm2 cells are necessary components for the computation of OFF motion signals. In line with this notion, we find both L4 and Tm2 neurons being excited preferentially by moving OFF edges. Furthermore, we demonstrate that direction selectivity does not occur at the level of L4 or Tm2 cells, but is rather computed downstream of Tm2, presumably in the dendrites of T5 cells.

Contrast Polarity and Direction Sensitivity

Using full-field flicker and moving edges of single contrast polarity, we measured the basic response characteristics of both L4 and Tm2 cells. L4 cells receive their main input from L2 in the lamina, where they form reciprocal, cholinergic connections [18, 21]. In agreement with previous studies [23, 28], we observed a decrease in Ca^{2+} when stimulating

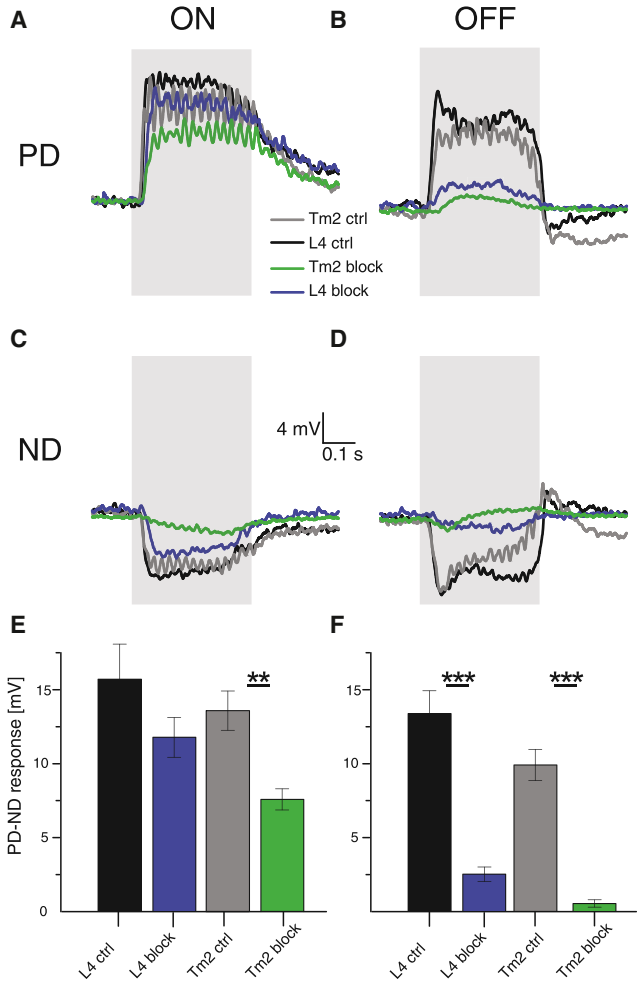

Figure 4. Voltage Responses of Lobula Plate Tangential Cells to Moving ON and OFF Edges

(A–D) Average time course of the membrane potential in response to ON (A and C) and OFF (B and D) edges moving along the preferred (PD; A and B) and null (ND; C and D) direction as recorded in two types of control flies (gray and black), as well as in flies in which synaptic output from L4 (blue) or Tm2 (green) cells was blocked. The stimulation period is indicated by the shaded area.

(E and F) Mean voltage responses (PD − ND) to ON (E) and OFF (F) edges of tangential cells in all four groups of flies. Recordings were done from HS [2] and VS [1] cells. HS cells have front to back as their PD and back to front as their ND; VS cells have downward as their PD and upward as their ND. Since no difference was detected between HS and VS cells, data from both cell types were pooled. L4 control data are from nine cells (four HS, five VS) in two flies, L4 block data are from ten cells (three HS, seven VS) in two flies, Tm2 control data are from 14 cells (six HS, eight VS) in eight flies, and Tm2 block data are from 11 cells (five HS, six VS) in five flies. In L4 block flies, ON responses are nonsignificantly different from control flies, whereas OFF responses are highly significantly reduced. In Tm2 block flies, ON responses are significantly different from control flies, and OFF responses are highly significantly reduced. *$p < 0.05$, **$p < 0.001$, ***$p < 0.0001$, tested using two-tailed t tests against their controls. Error bars indicate ±SEM.

See also Figures S1–S3.

L4 with brightness increments and an increase of Ca^{2+} when presenting light decrements. Assuming an excitatory connection between L2 and L4, these results are consistent with data that have been described for L2 [23, 26, 29]. The temporal response characteristics of L4, however, differ substantially from those observed in L2 by the existence of a sustained component in L4, which is not seen in L2. This discrepancy is in agreement with the finding that L4 receives input from photoreceptors, both directly from R6 and indirectly via the lamina amacrine cell, in addition to the input from L2 [22]. Tm2 receives its main input from L2. In agreement with this notion, we observed an increased Ca^{2+} signal in response to brightness decrements and no response to brightness increments. The transient nature of the signal and its selectivity for OFF edges parallels the reported findings for the Ca^{2+} signal in the terminal region of L2 [15, 29], suggesting that half-wave rectification in the L2 terminal represents the biophysical mechanism for OFF selectivity within the L2 pathway [29]. In contrast to L2, L4, and previous electrophysiological recordings in the calliphorid ortholog of Tm2 [28], Tm2 cells in *Drosophila* do not show any response to full-field luminance changes of either polarity. This finding indicates the existence of an inhibitory subregion of the receptive field. It also argues against the hypothesis that intercolumnar L4 connections onto Tm2 might implement a pooling of excitatory neighboring signals [18]. Furthermore, the observed nondirectional responses of both L4 and Tm2 allow us to rule out the hypothesis that the asymmetrical wiring between L4 and Tm2 could implement direction selectivity [18]. This passes the emergence of direction selectivity to the postsynaptic neurons—presumably T5—that have been shown to exhibit a precise directional tuning [12].

Receptive Field Properties

Stimulation with dark bars at different positions and increasing widths revealed the receptive field properties of L4 and Tm2 cells. We could demonstrate that the spatial sensitivity distribution for excitatory input to both cells exhibits comparable characteristics in the azimuthal extent when probed by small bars. However, it differs significantly in response to larger objects. Here, the response of L4 cells increases with the size of the visual stimulus, and thus varies distinctly from the center-surround receptive field described in L2 [26]. This is a further indication for a contribution of additional inputs to L4, e.g., via wide-field amacrine cells. As is shown by a linear receptive field model—an isotropic Gaussian inhibitory center with a half width σ of 2° and a spatially constant excitatory surround—even a minute excitatory surround contribution, undetectable by local stimulation, is sufficient to account for the increase in response with increasing stimulus size (Figure 5E). Tm2, in contrast, seems to be inhibited by large objects, since their response decreases dramatically when stimulated with bars wider than 4.5°. With Ca^{2+} as a proxy for membrane voltage, this inhibitory surround has not been detected by the stimulation with small bars at such lateral positions, either because intracellular Ca^{2+} does not decrease with membrane hyperpolarization or because the Ca^{2+} indicator does not report these low concentrations. Compared to L2 [26], surround inhibition seems to be much more pronounced in Tm2 (L2 responses from [26] are indicated as dashed line in Figure 3D). Tm2 cells lack every response to objects larger than 25°, indicating the existence of further lateral inhibition at the level of Tm2 that leads to a sharpening of their receptive field, probably via wide-field amacrine cells. In order to quantitatively reproduce Tm2 responses to bars of increasing width and moving gratings, we modeled the receptive field of Tm2 as the difference of two Gaussians with a half width σ of 2° horizontally and 4° vertically for the inhibitory center and of 10° horizontally and 20° vertically for the excitatory surround. This combination resulted in a maximum local surround excitation that amounted

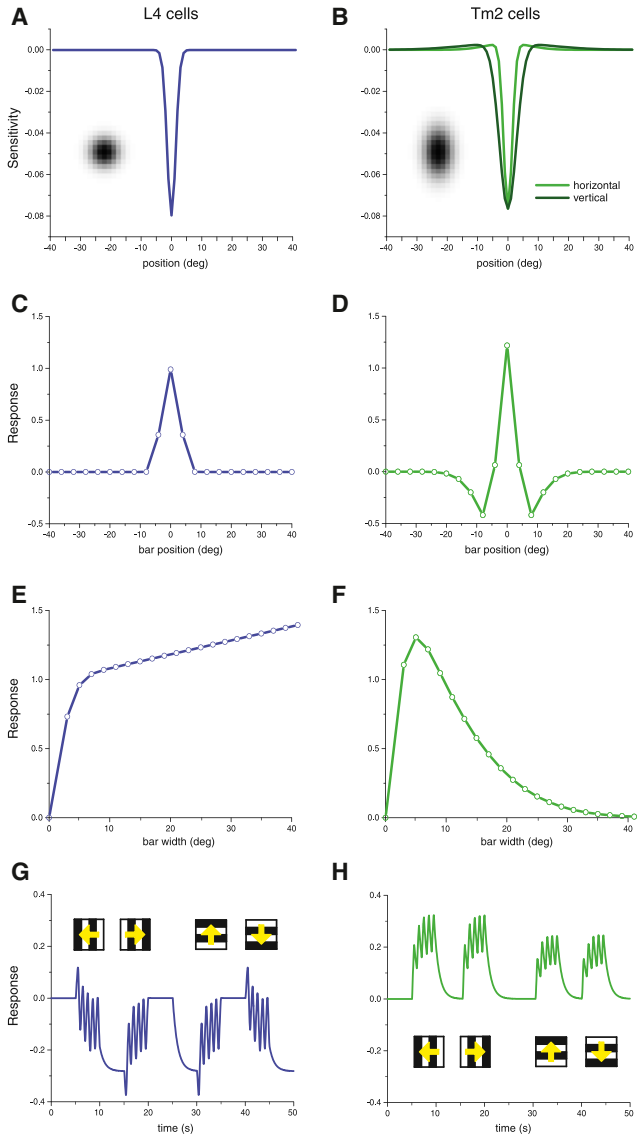

Figure 5. Model Simulations of L4 and Tm2 Receptive Fields

(A and B) Sensitivity profile across the receptive field of L4 (A) and Tm2 (B). The insets show a magnified view of the 2D receptive field, with each pixel corresponding to one $1^{\circ 2}$ of visual space.

(C and D) Responses of L4 (C) and Tm2 (D) to a 7°-wide bar as a function of bar position.

(E and F) Responses of L4 (E) and Tm2 (F) to a bar, centered in the receptive field, as a function of bar width.

(G and H) Responses of L4 (G) and Tm2 (H) to a grating (spatial wavelength = 20°) moving at a temporal frequency of 1 Hz along four orthogonal directions. Responses were obtained by low-pass filtering (τ = 1 s) of original signals from L4 and half-wave rectifying signals from Tm2.

See also Figure S3.

to only 3% of the peak center inhibition, but nevertheless was able to fully reproduce the strong decrease of the response of Tm2 with increasing bar width seen in the experiments (Figures 5B and 5F). A further interesting difference between L4 and Tm2 appears in their responses to moving square wave gratings: while L4 responses remain at rest, at best being slightly modulated at the temporal frequency of the local luminance changes (Figure 1E), Tm2 responses build up during grating motion with temporal modulations riding on top (Figure 1F). As shown by model simulations, these differences are readily explained by the half-wave rectified response property of Tm2, but not in L4, assuming a temporal integration of the membrane potential either by intracellular Ca^{2+} and/or the buffering of the indicator (Figures 5G and 5H). Furthermore, assuming a slight anisotropy of the receptive field of Tm2 as explained above (Figure 5B), similar to what has been reported for L2 [26], the simulation results for grating motion are consistent with the somewhat smaller response amplitude of Tm2 to vertical than to horizontal motion (Figure 5H). Note, however, that the anisotropy of the Tm2 receptive field was not directly measured.

L4 and Tm2 Are Crucial OFF Pathway Elements

To test the role of L4 and Tm2 in motion detection in *Drosophila*, we blocked their synaptic output and recorded from tangential cells of the lobula plate. Unlike a behavioral study by Silies and colleagues that shows only mild reductions in responses to OFF motion stimuli when blocking L4 [23], we observed a strong impairment of tangential cell responses for OFF motion. This difference might be explained by differing expression levels of Gal4 in L4 fly lines: in the same study, silencing L4 in two different fly lines caused significantly different effects of responses toward opposing edges [23]. In another study, Tuthill and colleagues tested the effect of blocking all lamina neurons individually on turning behavior of flying *Drosophilae* [24]. In agreement with our results, blocking L4 resulted in a selective impairment of the turning responses to OFF versus ON edges. In response to grating motion from the front to the back, these flies also exhibited a response reduction to about 50% of control level, as is expected from our data (Figures 4, S1, and S2). However, the same flies reacted with the same amplitude as control flies to grating motion from the back to the front. Since the behavioral response to back-to-front motion is much smaller than that to front-to-back motion, the residual tangential cell response might be sufficient to generate normal behavioral output under these conditions. Our results show that L4 is necessary for OFF motion signals in tangential cells (Figure 4). The same effect was observed when Tm2 was blocked. Blocking and Ca^{2+} imaging experiments match, because no direction-specific defect could be detected. This speaks in favor of the hypothesis that blocking Tm2 corresponds to the disruption of one input element to the Reichardt detector. L4, on the other hand, as one of the major input elements to Tm2 [18], seems to be needed either for a proper functioning of L2, or in conjunction with L2 to successfully evoke signals in Tm2. Our data also show a reduction in the responses of tangential cells in Tm2 block flies to ON stimuli, especially in the cells' null direction (Figure 4). This decrease of the ON response could be caused by disruption of a potential tonic input of Tm2 to the ON pathway via L5 [17, 18] or via its arborization in medulla layer 9. Together with the spatiotemporal response properties of Tm2 reported above, the following conclusions can be drawn regarding motion processing in the OFF pathway: (1) The narrow receptive field of Tm2 (Figure 3B) with a half width of about 5° indicates input from only a single optical cartridge. This is significantly smaller than the "anatomical receptive field," as reported in Takemura et al. [17] for Tm3, one of the inputs to the T4 cells, and thus might represent an interesting difference between the ON and the OFF motion pathway. (2) The strong surround inhibition we see in Tm2 (Figure 3D) readily explains the missing responses to field flicker stimuli that was observed in T5 cells

[12]. (3) The rather transient response of Tm2 (Figures 2B and 3F) makes it a candidate for the fast (i.e., high-pass filtered) input to the motion detection mechanism in the postsynaptic dendrite of T5 cells. This is all the more true since the calcium indicator is expected to slow down the signal significantly: thus, the membrane potential response in Tm2 will certainly be even faster. As a caveat, however, no data on Tm1 neurons exist so far to compare with. (4) The fact that blocking Tm2 abolishes the OFF response in the tangential cells for all stimulus directions (Figures 4B, 4D, and 4F) suggests that Tm2 serves as input element for all four types of T5 cells tuned to the four cardinal directions.

In summary, we thus conclude that L4 and Tm2 are essential OFF motion processing elements in the fly visual system that are not directionally selective. Consequently, direction selectivity in the OFF pathway is likely to arise at the level of the T5 dendrites.

Experimental Procedures

Flies

Flies were raised on standard cornmeal-agar medium with 12 hr light/12 hr dark cycles, 25°C, and 60% humidity. For Ca^{2+} imaging, we used the genetically encoded indicator GCaMP5 [30] driven by two different Gal4 lines with the following genotypes: $Tm2_{ca}$ line (*w^-;ort-Gal4-DBD,N9A≫BVP16-AD;UAS-GCaMP5*), provided by Chi-Hon Lee [31], and L4 line (*w^-;UAS-GCaMP5;VT40547-Gal4*, VDRC stock number 200265). Cell-specific block effects in electrophysiological experiments were accomplished using UAS-shibire^{ts} [27]. Fly lines with the following genotypes were used for electrophysiological recordings: L4 line (*shi^{ts}/+;+;shi^{ts}/VT40547-Gal4*, VDRC stock number 200265) and $Tm2_{el}$ line (*shi^{ts}/+;+;shi^{ts}/VT12282-Gal4*, VDRC stock number 203097). Expression and specificity of driver lines were investigated using a combination of membrane tethered GFP and synaptotagmin-hemagglutinin (courtesy of Andreas Prokop) [32, 33]. Fly lines had the following genotypes: $Tm2_{ca}$ line (*w^-;UAS-SYT-HA,UAS-mCD8-GFP/ort-Gal4-DBD,N9A≫BVP16-AD;+*), $Tm2_{el}$ line (*w^-;UAS-SYT-HA,UAS-mCD8-GFP/+;VT12282-Gal4/+*), and L4 line (*w^-;UAS-SYT-HA,UAS-mCD8-GFP/+;VT40547-Gal4/+*). The $Tm2_{ca}$ line had a higher Gal4 expression level than did the $Tm2_{el}$ line. The $Tm2_{el}$ line, however, showed a more specific expression pattern. Detailed descriptions of preparation and experiments are found in [29] for Ca^{2+} imaging and in [1] for electrophysiology.

Immunohistochemistry and Confocal Imaging

Immunostainings were performed as described in [2]. As primary antibodies (1:200) we used mouse anti-discs large (DLG, Developmental Studies Hybridoma Bank), rabbit anti-GFP-Alexa488 conjugate (Molecular Probes), and rat anti-hemagglutinin (Roche). For visualization, we used the following secondary antibodies (1:200 in PBT): goat anti-mouse Alexa 568, goat anti-rat Alexa 568 (Molecular Probes), and goat anti-mouse Alexa 647 (Rockland Immunochemicals). Brains were mounted (IMM, Ibidi) and optically sectioned in the horizontal plane with a Leica SP5 confocal microscope. For documentation, single sections were processed in ImageJ 1.46r (NIH).

Electrophysiology

The recording protocol was adapted from [1]. In addition, the glial sheet was digested locally by application of a stream of 0.5 mg/ml collagenase IV (GIBCO) through a cleaning micropipette (~5 μm opening) under polarized light contrast.

Two-Photon Microscopy and Visual Stimulation

Two-photon microscopy and visual stimulus presentation were performed as described in [12]. Square-wave gratings had a spatial wavelength of 30° of visual angle and a contrast of 88%, moving at either 30° s^{-1} or 60° s^{-1}. Edges had the same contrast and were moving at 30° s^{-1}. For the experiments shown in Figures 1 and 2, each grating or edge motion was shown twice within a single sweep, each lasting 4 s. Subsequent stimuli were preceded by a 3 s pause. For the experiments shown in Figures 3A and 3B, we flickered 4.5°-wide vertical dark bars on a bright background at 0.5 Hz at 10 different positions. The position yielding maximum response was set to 0°. The responses were normalized and plotted depending on their distance to the peak response. For Figures 3C and 3D, vertical dark bars, increasing in size, were flickered at the peak response position. The responses were normalized to the peak response. For Figures 3E and 3F, a 4.5° vertical dark bar was flickered for 1 s on a bright background (line scan, averaged trace, ten repetitions). For the experiments shown in Figure 4, multiple edges were used as stimuli moving simultaneously at 60° s^{-1}. For stimulation of HS cells, a vertical, stationary square-wave grating with 45° spatial wavelength was presented. For ON edge motion, the right (PD) or the left (ND) edge of each light bar started moving until it merged with the neighboring bar. For OFF edge motion, the right or the left edge of each dark bar was moving. For stimulation of VS cells, the pattern was rotated by 90°. A collection of all stimuli is presented as space-time plots in Figure S3.

Data Evaluation

Data were evaluated offline using custom written software (MATLAB) and Origin (OriginLab). For evaluation of the Ca^{2+} imaging data, the raw image series was first converted into a relative fluorescence change (ΔF/F) series using the first five images as reference. Then a region was defined within a raw image and average ΔF/F values were determined within that region for each image, resulting in a ΔF/F signal over time. The Ca^{2+} signal traces in Figures 1C–1F were obtained by calculation of the average ΔF/F signal over trials and flies, with shading indicating the SEM. For the bar graphs in Figure 2C, the average signals of three frames before stimulus onset were subtracted from the mean response within the three last images of edge motion. For Figure 2D, the average Ca^{2+} signal of three images prior to visual stimulation (reference value) was subtracted from the maximum response during each stimulus presentation. The dashed line was calculated by subtraction of the reference value from a maximum, obtained without visual stimulation (chance response level). The graphs in Figures 3A and 3B show the average signal (maximum − minimum of peaks, five presentations) to flickering bars normalized to the maximum response. Again, the dashed line represents chance level. The voltage traces in Figures 4A–4D were obtained by averaging of the responses of all cells upon visual stimulation with multiple edges of either polarity in the four cardinal directions. For the bar graphs in Figures 4E and 4F, the responses during edge motion (0.375 s) along the preferred and null direction were subtracted (PD − ND). The mean PD − ND responses were subsequently averaged across all cells, with error bars representing the SEM.

Supplemental Information

Supplemental Information includes three figures and can be found with this article online at http://dx.doi.org/10.1016/j.cub.2014.01.006.

Acknowledgments

We thank Chi-Hon Lee and Andreas Prokop for providing us with fly lines; David Soll for the Dlg-antibody; Johannes Plett for designing and engineering the LED arena and for technical support; Christian Theile, Wolfgang Essbauer, and Michael Sauter for fly work; Romina Kutlesa for stainings; and Aljoscha Leonhardt, Elisabeth Hopp, and Georg Ammer for constructive discussions and help with programming.

Received: October 22, 2013
Revised: November 29, 2013
Accepted: January 3, 2014
Published: February 6, 2014

References

1. Joesch, M., Plett, J., Borst, A., and Reiff, D.F. (2008). Response properties of motion-sensitive visual interneurons in the lobula plate of Drosophila melanogaster. Curr. Biol. *18*, 368–374.
2. Schnell, B., Joesch, M., Forstner, F., Raghu, S.V., Otsuna, H., Ito, K., Borst, A., and Reiff, D.F. (2010). Processing of horizontal optic flow in three visual interneurons of the Drosophila brain. J. Neurophysiol. *103*, 1646–1657.
3. Hassenstein, B., and Reichardt, W. (1956). Systemtheoretische Analyse der Zeit-, Reihenfolgen- und Vorzeichenauswertung bei der Bewegungsperzeption des Rüsselkäfers Chlorophanus. Z. Naturforsch. B *11b*, 513–524.
4. Reichardt, W. (1987). Computation of optical motion by movement detectors. J. Comp. Physiol. A *161*, 533–547.

5. Borst, A., and Euler, T. (2011). Seeing things in motion: models, circuits, and mechanisms. Neuron *71*, 974–994.
6. Fischbach, K., and Dittrich, A. (1989). The optic lobe of Drosophila melanogaster. I. A Golgi analysis of wild-type structure. Cell Tissue Res. *258*, 441–475.
7. Bausenwein, B., Dittrich, A.P.M., and Fischbach, K.F. (1992). The optic lobe of Drosophila melanogaster. II. Sorting of retinotopic pathways in the medulla. Cell Tissue Res. *267*, 17–28.
8. Bausenwein, B., and Fischbach, K.F. (1992). Activity labeling patterns in the medulla of Drosophila melanogaster caused by motion stimuli. Cell Tissue Res. *270*, 25–35.
9. Rister, J., Pauls, D., Schnell, B., Ting, C.Y., Lee, C.H., Sinakevitch, I., Morante, J., Strausfeld, N.J., Ito, K., and Heisenberg, M. (2007). Dissection of the peripheral motion channel in the visual system of *Drosophila melanogaster*. Neuron *56*, 155–170.
10. Joesch, M., Schnell, B., Raghu, S.V., Reiff, D.F., and Borst, A. (2010). ON and OFF pathways in Drosophila motion vision. Nature *468*, 300–304.
11. Buchner, E., Buchner, S., and Bülthoff, I. (1984). Deoxyglucose mapping of nervous activity induced in Drosophila brain by visual movement. J. Comp. Physiol. *155*, 471–483.
12. Maisak, M.S., Haag, J., Ammer, G., Serbe, E., Meier, M., Leonhardt, A., Schilling, T., Bahl, A., Rubin, G.M., Nern, A., et al. (2013). A directional tuning map of Drosophila elementary motion detectors. Nature *500*, 212–216.
13. Schnell, B., Raghu, S.V., Nern, A., and Borst, A. (2012). Columnar cells necessary for motion responses of wide-field visual interneurons in Drosophila. J. Comp. Physiol. A Neuroethol. Sens. Neural Behav. Physiol. *198*, 389–395.
14. Eichner, H., Joesch, M., Schnell, B., Reiff, D.F., and Borst, A. (2011). Internal structure of the fly elementary motion detector. Neuron *70*, 1155–1164.
15. Clark, D.A., Bursztyn, L., Horowitz, M.A., Schnitzer, M.J., and Clandinin, T.R. (2011). Defining the computational structure of the motion detector in Drosophila. Neuron *70*, 1165–1177.
16. Joesch, M., Weber, F., Eichner, H., and Borst, A. (2013). Functional specialization of parallel motion detection circuits in the fly. J. Neurosci. *33*, 902–905.
17. Takemura, S.Y., Bharioke, A., Lu, Z., Nern, A., Vitaladevuni, S., Rivlin, P.K., Katz, W.T., Olbris, D.J., Plaza, S.M., Winston, P., et al. (2013). A visual motion detection circuit suggested by Drosophila connectomics. Nature *500*, 175–181.
18. Takemura, S.Y., Karuppudurai, T., Ting, C.-Y., Lu, Z., Lee, C.-H., and Meinertzhagen, I.A. (2011). Cholinergic circuits integrate neighboring visual signals in a Drosophila motion detection pathway. Curr. Biol. *21*, 2077–2084.
19. Braitenberg, V., and Debbage, P. (1974). A regular net of reciprocal synapses in the visual system of the fly, Musca domestica. J. Comp. Physiol. *90*, 25–31.
20. Strausfeld, N.J., and Campos-Ortega, J.A. (1973). The L4 monopolar neurone: a substrate for lateral interaction in the visual system of the fly Musca domestica (L.). Brain Res. *59*, 97–117.
21. Meinertzhagen, I.A., and O'Neil, S.D. (1991). Synaptic organization of columnar elements in the lamina of the wild type in Drosophila melanogaster. J. Comp. Neurol. *305*, 232–263.
22. Rivera-Alba, M., Vitaladevuni, S.N., Mishchenko, Y., Lu, Z., Takemura, S.Y., Scheffer, L., Meinertzhagen, I.A., Chklovskii, D.B., and de Polavieja, G.G. (2011). Wiring economy and volume exclusion determine neuronal placement in the Drosophila brain. Curr. Biol. *21*, 2000–2005.
23. Silies, M., Gohl, D.M., Fisher, Y.E., Freifeld, L., Clark, D.A., and Clandinin, T.R. (2013). Modular use of peripheral input channels tunes motion-detecting circuitry. Neuron *79*, 111–127.
24. Tuthill, J.C., Nern, A., Holtz, S.L., Rubin, G.M., and Reiser, M.B. (2013). Contributions of the 12 neuron classes in the fly lamina to motion vision. Neuron *79*, 128–140.
25. Denk, W., Strickler, J.H., and Webb, W.W. (1990). Two-photon laser scanning fluorescence microscopy. Science *248*, 73–76.
26. Freifeld, L., Clark, D.A., Schnitzer, M.J., Horowitz, M.A., and Clandinin, T.R. (2013). GABAergic lateral interactions tune the early stages of visual processing in Drosophila. Neuron *78*, 1075–1089.
27. Kitamoto, T. (2001). Conditional modification of behavior in Drosophila by targeted expression of a temperature-sensitive shibire allele in defined neurons. J. Neurobiol. *47*, 81–92.
28. Douglass, J.K., and Strausfeld, N.J. (1995). Visual motion detection circuits in flies: peripheral motion computation by identified small-field retinotopic neurons. J. Neurosci. *15*, 5596–5611.
29. Reiff, D.F., Plett, J., Mank, M., Griesbeck, O., and Borst, A. (2010). Visualizing retinotopic half-wave rectified input to the motion detection circuitry of Drosophila. Nat. Neurosci. *13*, 973–978.
30. Akerboom, J., Chen, T.-W., Wardill, T.J., Tian, L., Marvin, J.S., Mutlu, S., Calderón, N.C., Esposti, F., Borghuis, B.G., Sun, X.R., et al. (2012). Optimization of a GCaMP calcium indicator for neural activity imaging. J. Neurosci. *32*, 13819–13840.
31. Ting, C.-Y., Gu, S., Guttikonda, S., Lin, T.-Y., White, B.H., and Lee, C.-H. (2011). Focusing transgene expression in Drosophila by coupling Gal4 with a novel split-LexA expression system. Genetics *188*, 229–233.
32. Löhr, R., Godenschwege, T., Buchner, E., and Prokop, A. (2002). Compartmentalization of central neurons in Drosophila: a new strategy of mosaic analysis reveals localization of presynaptic sites to specific segments of neurites. J. Neurosci. *22*, 10357–10367.
33. Robinson, I.M., Ranjan, R., and Schwarz, T.L. (2002). Synaptotagmins I and IV promote transmitter release independently of Ca(2+) binding in the C(2)A domain. Nature *418*, 336–340.